

Using matrix projection model to predict climate-induced range expansion/contraction for a dioecious range-limited species

Jacob K. Moutouama¹, Aldo Compagnoni², and Tom E.X. Miller¹

¹Program in Ecology and Evolutionary Biology, Department of BioSciences, Rice
University, Houston, TX USA

²Institute of Biology, Martin Luther University Halle-Wittenberg, Halle,
Germany; and German Centre for Integrative Biodiversity Research (iDiv),
Leipzig, Germany

July 31, 2023

* Corresponding author: jmoutouama@gmail.com

Submitted to *Ecological Monographs*

Manuscript type: Article

Open Research statement: All of our data and code are available during peer review at
<https://github.com/jmoutouama/POAR-Forecasting>. This manuscript and its contents
can be reproduced from this file: <https://github.com/jmoutouama/POAR-Forecasting/>
Manuscript/Forescasting.Rnw. All data are provided at <https://github.com/jmoutouama/>
POAR-Forecasting/tree/main/data.

1

Abstract

2

Keywords

2

Introduction

Rising temperatures and extreme drought events have already caused broad-scale vulnerability of native species, leading to increased concern about how species will redistribute across the globe under future climate conditions. Dioecious species might be particularly vulnerable to climate change because they often display skewed sex ratios that are reinforced by differentiation of sexual niches (Tognetti, 2012). Accounting for such a niche differentiation between male and female within a population is a long-standing challenge in accurately predicting which sex will successfully track environmental change and how this will impact population dynamics (Jones et al., 1999). As a result, accurate forecasts of colonization-extinction dynamics for dioecious species under future climate scenarios are limited.

The effect of climate conditions on species distributions is often derived by correlative relationships between species occurrence record or abundance patterns and current climate conditions (Elith and Leathwick, 2009). These established relationships serve as the basis for predicting how species will redistribute across the globe in a changing world. However, the responsiveness of species abundance patterns often lags behind environmental change, which can lead to pronounced mismatches in current and future climate conditions and colonization-extinction dynamics (Lee-Yaw et al., 2022).

More recently, "mechanistic approach" of species distribution model (SDM) and trait based species distribution modeling approach have been proposed as alternatives to the correlative approach of SDM (Porter et al., 2010; Kearney and Porter, 2009; Benito Garzón et al., 2019). Although the application of these approaches has been successful for some species, they present several challenges. 'Mechanistic approaches' of SDM require information on individual physiological parameters (thermal conductivity, oxygen extraction

efficiency, stomatal conductance, water exchange) that is not often available for most species (Daley and Phillips, 2006; Peterson et al., 2015). Trait-based SDM is estimated from a network on common gardens, that are not also available for most species. When available, these common gardens allow the estimation of traits that are related only to the survival part of fitness (Benito Garzón et al., 2019).

Theory predicts that if the cost of reproduction for each sex is equal and if males and females differ in reproductive fitness equality with increasing size, then natural selection will act to balance a population sex ratio at 1:1 (Fisher, 1930). However, deviances from those assumptions have been observed. In several plant species, females are more sensitive to stress-related resource availability conditions than males, leading to high female mortality and, therefore, to a male bias sex ratio (Hultine et al., 2016). Furthermore, the lower cost of reproduction of males may allow them to invest their energy in other functions that produce higher growth rates, higher clonality, or even higher survival rates compared to females (Bruijning et al., 2017), causing a skew sex ratio.

Climate change could therefore magnify skewed sex ratios and potentially reduced population growth rate if individuals are unable to find a mate and reproduce (Morrison et al., 2016). In reverse, dioecious species could also adapt to climate change. For instance, as the drier, warmer climate moves “up slope”, so will adapt arid males shifting the sex ratios (Petry et al., 2016). Because of this, populations in which males are rare under current climatic conditions could experience less mate limitation, allowing females to successfully produce more seed under warmer conditions and favor range shifts in response (Petry et al., 2016). However, due to the difficulty in experimentally addressing how dioecious species respond demographically to climate change, most studies often focused only on how climate change affects the sex ratio and rarely on the impact of climate change on the population dynamics of dioecious species and its implications for

52 range shifts.

53 Our ability to track the impact of climate change on the population dynamics of dioe-
54 cious plants depends on our ability to build mechanistic models that take into account
55 the spatial and temporal context in which survival, reproduction, and growth occur due
56 to the sessile nature of these plants (Czachura and Miller, 2020). Several studies found
57 that climate change affects demographic processes in distinctive and potentially contrast-
58 ing ways (Dalgleish et al., 2011). For example, while climate has a significant effect on
59 the probability of survival and growth, it has no effect on the probability of flowering
60 (Greiser et al., 2020). Additionally, under warmer conditions, some native species will
61 fail to establish reproductive populations due to the extremely low germination rate and
62 seedling survival (Reed et al., 2021a). Therefore, climate change will reduce the popula-
63 tion growth rate and the range size of these species (Reed et al., 2021b). Other species will
64 persist or even increase their range in response to climate change (Williams et al., 2015;
65 Merow et al., 2017). In seabird populations, climate change by increasing the survival
66 rate of both sexes favored their population growth rate (Gianuca et al., 2019).

67 In this study, we used a matrice projection model to understand the demographic
68 response of dioecious species to climate change and its implications on range dynamics.
69 Our study system is a dioecious plant species (*Poa arachnifera*) distributed along an arid-
70 ity gradient. A previous study on the system showed that, despite the differentiation
71 of the niche between sexes, the female niche mattered the most in driving the environ-
72 mental limits of the viability of *Poa arachnifera* populations (Miller and Compagnoni,
73 2022). Thus, under current climate conditions, we hypothesized that high temperature
74 and lower precipitation during the growing season have negative effects on population
75 growth rate through a reduction in female growth, survival, and fecundity rate. How-
76 ever, that reduction in population growth rate will not go below a viable population

77 (population growth rate less than one) even at range edge. Future climate will exacerbate
78 the effect of temperature and precipitation on female vital rates and drive population to
79 extinction, particularly at range edge.

80

Materials and methods

81

Study system

82 Texas blue grass (*Poa arachnifera*) is a perennial cool season plant. The species occurs in
83 Texas, Oklahoma, and Southern Kansas (Hitchcock, 1971). Texas blue produces a dark
84 green ground cover throughout the summer between October and May, with onset of
85 dormancy often from June to September (Kindiger, 2004). When flowering, males often
86 have anthers, and females have stigmas. The species is pollinated by wind (Hitchcock,
87 1971).

88 We studied 14 sites along the distribution of these species in the United States in 2014
89 and 2015.

90

Demographic and climatic data collection

91 In each site we collected individual demographic data including survival, growth (number
92 of tillers), flowers and fertility (number of panicle) for two censuses (2015 and 2016)
93 to build our demographic models. The details of the data collection has been provided
94 in Miller and Compagnoni (2022).

95 We want to understand how current and future climate affect the dynamic of *Poa*
96 *arachnifera*. Therefore, we considered the climatic data from the time we collected demo-
97 graphic data (2015 and 2016 censuses) as the current condition for the species. Addition-
98 ally, months were aligned to match demographic transition years rather than calendar

99 years. The monthly temperature and precipitation data were downloaded for each site
100 from Chelsea (Karger et al., 2017). We define June to September as the dormant sea-
101 son of the year and the rest of the year as the growing season. We preferred seasonal
102 data because they allowed us to quantify the response of species to change in seasonal
103 change in climate. We evaluated future climate projections from two scenarios: SSP 370,
104 an intermediate-to-pessimistic scenario assuming a radiative forcing to amount to 7.0
105 Wm^{-2} by 2100, and SSP 585, a pessimistic emission scenario which project a radiative
106 forcing to amount to 8.5 Wm^{-2} by 2100 (O'Neill et al., 2017; Brun et al., 2022). The pre-
107 cipitation of growing season and dormant season were not explained by the Temperature
108 of growing season and dormant season ([Appendix S1: Figure S1](#)).

109 *Sex ratio experiment*

110 We also conducted a sex-ratio experiment to measure the effect of male panicle avail-
111 ability on seed viability on females panicles. Details of the experiment are provided in
112 Compagnoni et al. (2017) and Miller and Compagnoni (2022).

113 We used the sex-ratio to estimate the probability of viability and the germination
114 rate. Seed viability was modeled with a binomial distribution where the probability of
115 viability (v) was given by:

$$v = v_0 * (1 - OSR^\alpha) \quad (1)$$

116 where OSR is the operational sex ratio (proportion of panicles that were female) in the
117 experimental populations. The properties of the above function is supported by our
118 previous work (Compagnoni et al., 2017). Here, seed viability is maximized at v_0 as OSR
119 approaches zero (strongly male-biased) and goes to zero as OSR approaches 1 (strongly

120 female-biased). Parameter α controls how viability declines with increasing female bias.
121 We used a binomial successes to model the germination data from greenhouse trials.
122 Given that, germination was conditional on seed viability, the probability of success was
123 given by the product $v * g$, where v is a function of OSR (Eq. 1) and g is assumed to be
124 constant.

125 *Vital rate responses to climate*

126 We used individual level measurements of survival, growth (number of tillers), flow-
127 ering, number of panicle to independently develop two Bayesian mixed effect models
128 describing how each vital rate varies as a function of size, precipitation of growing and
129 dormant season and temperature of of growing and dormant season. The first one was
130 a linear, and the second one was a second-degree polynomial. We included a second-
131 degree polynomial because we expected that climate variables would affect vital rates
132 through a hump-shaped relationship, estimated via linear and quadratic terms, whereby
133 low value of climatic variables promote low survival, growth, and fertility probability ,
134 intermediate value of climate variable drives high probability of survival, growth, and
135 fertility probability, and high value of climate variable drives a decrease of probability of
136 survival, growth, and fertility probability. In each model, we used the temperature and
137 precipitation of the growing season and dormant season and individual size as predic-
138 tors. We centered and standardized all predictors to facilitate model convergence. We
139 included site, source, and block as random effect. All the vital rate models used the
140 same linear and quadratic predictor for the expected value (μ). However, we applied a
141 different link function ($f(\mu)$) depending on the distribution the vital rate ([Appendix S1:](#)
142 [Section S1](#)). We modeled survival and flowering data with a Bernoulli distribution. We
143 modeled the growth (tiller number) with a zero-truncated Poisson inverse Gaussian dis-

144 tribution. Fertility (panicle count) was model as zero-truncated negative binomial. We
145 fit all models in Stan (Stan Development Team, 2023), with weakly informative priors for
146 coefficients ($\mu = 0, \sigma = 100$) and variances ($\gamma[0.001, 0.001]$). We ran three chains for 1000
147 samples for warmup and 40000 for interactions, with a thinning rate of 3. We accessed
148 the quality of the models using trace plots and predictive check graphs ([Appendix S1: Figure S1](#)). Then, we used approximate Bayesian leave-one-out cross-validation (LOOIC)
149 to select the best model describing the effect of climate variable on vital rate. The final
150 model was the model with the lowest LOOIC (Vehtari et al., 2017).
151

152 To understand the effect of climate on vital rates, we used the 95 % credible interval
153 of the final model for each vital rate. When the 95 % credible interval of the coefficient
154 of a given climatic variable did not include zero, we concluded that there is a strong
155 effect of that variable on the vital rate. In contrast, when we have a credible interval of
156 a climatic variable that includes zero, we used the empirical cumulative distribution to
157 find the probability that the coefficient of that climatic variable is greater than zero.

158 *Population growth rate responses to climate*

159 To understand the effect of climate on population growth rate, we used the vital rate
160 estimated earlier to built a matrix projection model (MPM) structured by size (number of
161 tillers) and sex with "Climate" as covariate. For a given climatic variable, let $F_{x,t}$ and $M_{x,t}$
162 be the number of female and male plants of size x in year t , where $x \in \{1, 2, \dots, U\}$ and
163 U is the maximum number of tillers a plant can reach (here 99th percentile of observed
164 maximum size). Let F_t^R and M_t^R be the new recruits, which we assume do not reproduce
165 in their first year. We assume that the parameters of sex ratio-dependent mating (Eq. 1)
166 do not vary with climate. For a pre-breeding census, the expected numbers of recruits in

¹⁶⁷ year $t + 1$ is given by:

$$F_{t+1}^R = \sum_{x=1}^U [p^F(x) \cdot c^F(x) \cdot d \cdot v(\mathbf{F}_t, \mathbf{M}_t) \cdot m \cdot \rho] F_{x,t} \quad (2)$$

$$M_{t+1}^R = \sum_{x=1}^U [p^F(x) \cdot c^F(x) \cdot d \cdot v(\mathbf{F}_t, \mathbf{M}_t) \cdot m \cdot (1 - \rho)] F_{x,t} \quad (3)$$

¹⁶⁸ where p^F and c^F are flowering probability and panicle production for females of size x ,
¹⁶⁹ d is the number of seeds per female panicle, v is the probability that a seed is fertilized,
¹⁷⁰ m is the probability that a fertilized seed germinates, and ρ is the primary sex ratio
¹⁷¹ (proportion of recruits that are female). Seed fertilization depends on the OSR of panicles
¹⁷² (following Eq. 1) which was derived from the $U \times 1$ vectors of population structure \mathbf{F}_t
¹⁷³ and \mathbf{M}_t :

$$v(\mathbf{F}_t, \mathbf{M}_t) = v_0 * \left[1 - \left(\frac{\sum_{x=1}^U p^F(x) c^F(x) F_{x,t}}{\sum_{x=1}^U p^F(x) c^F(x) F_{x,t} + p^M(x) c^M(x) M_{x,t}} \right)^\alpha \right] \quad (4)$$

¹⁷⁴ Thus, the dynamics of the size-structured component of the population are given by:

$$F_{y,t+1} = [\sigma \cdot g^F(y, x = 1)] F_t^R + \sum_{x=1}^U [s^F(x) \cdot g^F(y, x)] F_{x,t} \quad (5)$$

$$M_{y,t+1} = [\sigma \cdot g^M(y, x = 1)] M_t^R + \sum_{x=1}^U [s^M(x) \cdot g^M(y, x)] M_{x,t} \quad (6)$$

¹⁷⁵ In the two formula above, the first term represents seedlings that survived their first
¹⁷⁶ year and enter the size distribution of established plants. Instead of using *P. arachnifera*
¹⁷⁷ survival probability, we used the seedling survival probability (σ) from demographic
¹⁷⁸ studies of a sister species hermaphroditic, *Poa autumnalis* in east Texas (T.E.X. Miller
¹⁷⁹ and J.A. Rudgers, *unpublished data*), and we assume this probability was constant across
¹⁸⁰ sexes and climatic variables. We did this because we had little information on the early

181 life cycle transitions of greenhouse-raised transplants. We also assume that $g(y, x =$
182 1) is the probability that a surviving seedlings reach size y , the expected future size
183 of 1-tiller plants from the transplant experiment. The second term represents survival
184 and size transition of established plants from the previous year, where s and g give
185 the probabilities of surviving at size x and growing from sizes x to y , respectively, and
186 superscripts indicate that these functions may be unique to females (F) and males (M).

187 Because the two-sex MPM is nonlinear (vital rates affect and are affected by popu-
188 lation structure) we estimated the asymptotic geometric growth rate (λ) by numerical
189 simulation, and repeated this across a range of climate.

190 *Identifying the mechanisms of population growth rate sensitivity to
191 climate*

192 To identify the mechanism by which climate affects population growth rate, we decom-
193 posed the effect of each climate variable (here Climate) on population growth rate (λ)
194 into contribution arising from the effect on each stage-specific vital rate (Caswell, 2000).
195 At this end we used a life table response experiment (LTRE) with a regression designs.
196 The LTRE approximates the change in λ with climate as the product of the sensitivity of
197 λ to the parameters times the sensitivity of the parameters to climate, summed over all
198 parameters (Caswell, 1989):

$$\frac{\partial \lambda}{\partial \text{Climate}} \approx \sum_i \frac{\partial \lambda}{\partial \theta_i^F} \frac{\partial \theta_i^F}{\partial \text{Climate}} + \frac{\partial \lambda}{\partial \theta_i^M} \frac{\partial \theta_i^M}{\partial \text{Climate}} \quad (7)$$

199 where, θ_i^F and θ_i^M represent sex-specific parameters: the regression coefficients for the
200 intercepts and slopes of size-dependent vital rate functions. Because LTRE contributions
201 are additive, we summed across vital rates to compare the total contributions of female

202 and male parameters.

203 *Implication on niche breath and range expansion/contraction*

204 To understand the implication of our study on niche breath, we projected the population
205 growth current and future prediction on two axes of climatic conditions (temperature
206 and precipitation) of each seasonal season (dormant and growing season). Similarly, to
207 understand the implication of our study on range contraction on expansion, we extrap-
208 olate population growth current and future prediction across the range to map species
209 distributions.

210 All the analysis were performed in R 4.3.1 (R Core Team, 2023)

Appendix S1

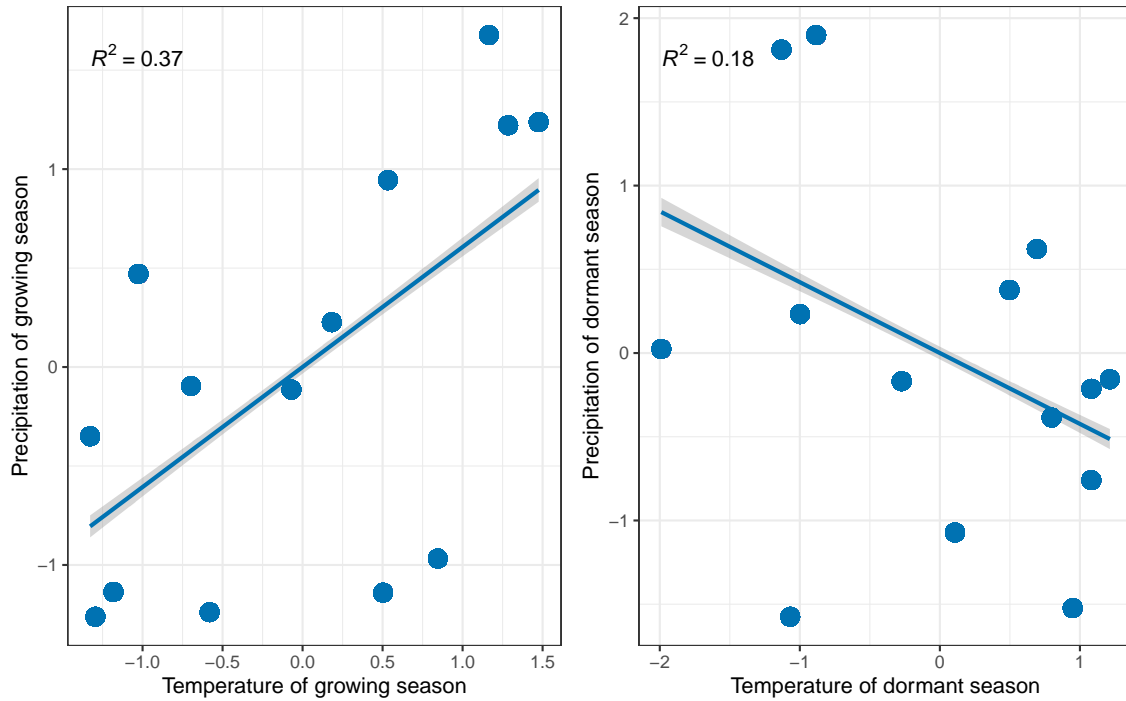


Figure S1: Relation between precipitation and temperature for each season (growing and dormant). R^2 indicates the value of proportion of explained variance between the temperature and precipitation

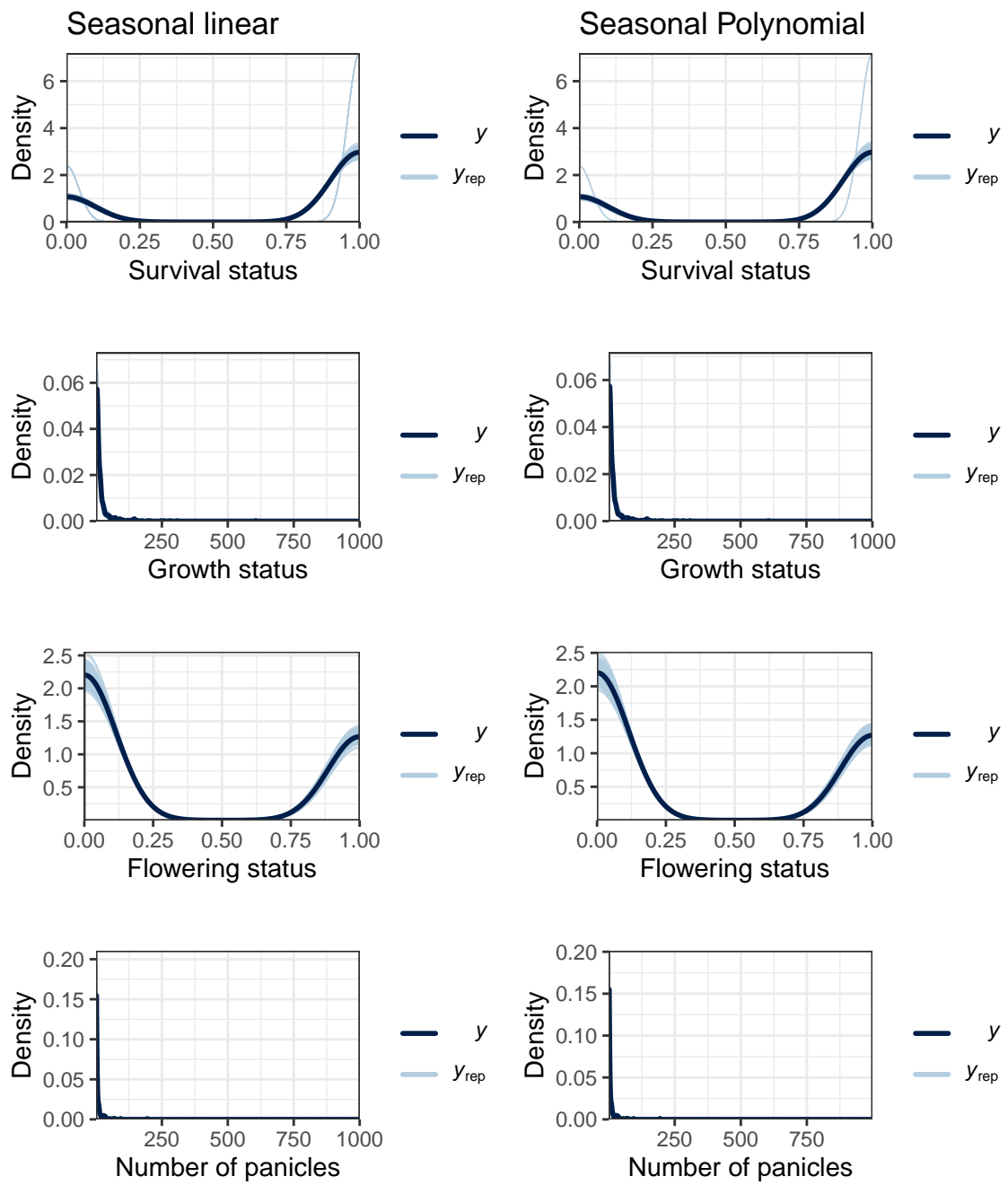


Figure S2: Consistency between real data and simulated values suggests that the fitted model accurately describes the data. Graph shows density curves for the observed data (light blue) along with the simulated values (dark blue). The first column shows the linear models and the second column shows the 2 degree polynomial models.

212

Section S1

$$S \sim Bernoulli(\hat{S}) \quad (1a)$$

$$F \sim Bernoulli(\hat{F}) \quad (1b)$$

$$G \sim Zero-truncated Poisson inverse Gaussian(\hat{G}) \quad (1c)$$

$$Fer \sim Zero-truncated negative binomial(\hat{Fer}) \quad (1d)$$

213

$$\hat{S} = \frac{\exp(f(\mu))}{1 + \exp(f(\mu))} \quad (2a)$$

$$\hat{F} = \frac{\exp(f(\mu))}{1 + \exp(f(\mu))} \quad (2b)$$

$$\hat{G} = \exp(f(\mu)) \quad (2c)$$

$$\hat{Fer} = \exp(f(\mu)) \quad (2d)$$

214

$$\begin{aligned}
f(\mu) = & \beta_0 + \beta_1 size + \beta_2 sex + \beta_3 pptgrow + \beta_4 pptdorm + \beta_5 tempgrow \\
& + \beta_6 tempdorm + \beta_7 pptgrow * sex + \beta_8 pptdorm * sex + \beta_9 tempgrow * sex \\
& + \beta_{10} tempdorm * sex + \beta_{11} size * sex + \beta_{12} pptgrow * tempgrow \\
& + \beta_{13} pptdorm * tempdorm + \beta_{14} pptgrow * tempgrow * sex \\
& + \beta_{15} pptdorm * tempdorm * sex + \beta_{16} pptgrow^2 + \beta_{17} pptdorm^2 \\
& + \beta_{18} tempgrow^2 + \beta_{19} tempdorm^2 + \beta_{20} pptgrow^2 * sex \\
& + \beta_{21} pptdorm^2 * sex + \beta_{22} tempgrow^2 * sex \\
& + \beta_{23} tempdorm^2 * sex + \phi + \rho + \nu
\end{aligned} \tag{3}$$

215

Literature Cited

- 216 Benito Garzón, M., T. M. Robson, and A. Hampe. 2019. Δ Trait SDMs: species distribution
217 models that account for local adaptation and phenotypic plasticity. *New Phytologist*
218 **222**:1757–1765.
- 219 Bruijning, M., M. D. Visser, H. C. Muller-Landau, S. J. Wright, L. S. Comita, S. P. Hubbell,
220 H. de Kroon, and E. Jongejans. 2017. Surviving in a cosexual world: A cost-benefit
221 analysis of dioecy in tropical trees. *The American Naturalist* **189**:297–314.
- 222 Brun, P., N. E. Zimmermann, C. Hari, L. Pellissier, and D. N. Karger. 2022. Global climate-
223 related predictors at kilometer resolution for the past and future. *Earth System Science
224 Data* **14**:5573–5603.
- 225 Caswell, H. 1989. Analysis of life table response experiments I. Decomposition of effects
226 on population growth rate. *Ecological Modelling* **46**:221–237.
- 227 Caswell, H. 2000. Matrix population models. Sinauer Sunderland, MA.
- 228 Compagnoni, A., K. Steigman, and T. E. Miller. 2017. Can't live with them, can't live
229 without them? Balancing mating and competition in two-sex populations. *Proceedings
230 of the Royal Society B: Biological Sciences* **284**:20171999.
- 231 Czachura, K., and T. E. Miller. 2020. Demographic back-casting reveals that subtle
232 dimensions of climate change have strong effects on population viability. *Journal of
233 Ecology* **108**:2557–2570.
- 234 Daley, M. J., and N. G. Phillips. 2006. Interspecific variation in nighttime transpiration
235 and stomatal conductance in a mixed New England deciduous forest. *Tree physiology*
236 **26**:411–419.

- 237 Dalgleish, H. J., D. N. Koons, M. B. Hooten, C. A. Moffet, and P. B. Adler. 2011. Climate
238 influences the demography of three dominant sagebrush steppe plants. *Ecology* **92**:75–
239 85.
- 240 Elith, J., and J. R. Leathwick. 2009. Species distribution models: ecological explana-
241 tion and prediction across space and time. *Annual review of ecology, evolution, and*
242 *systematics* **40**:677–697.
- 243 Fisher, R. A. 1930. The genetical theory of natural selection .
- 244 Gianuca, D., S. C. Votier, D. Pardo, A. G. Wood, R. B. Sherley, L. Ireland, R. Choquet,
245 R. Pradel, S. Townley, J. Forcada, et al. 2019. Sex-specific effects of fisheries and
246 climate on the demography of sexually dimorphic seabirds. *Journal of Animal Ecology*
247 **88**:1366–1378.
- 248 Greiser, C., K. Hylander, E. Meineri, M. Luoto, and J. Ehrlén. 2020. Climate limitation
249 at the cold edge: contrasting perspectives from species distribution modelling and a
250 transplant experiment. *Ecography* **43**:637–647.
- 251 Hitchcock, A. S. 1971. Manual of the grasses of the United States. Courier Corporation.
- 252 Hultine, K. R., K. C. Grady, T. E. Wood, S. M. Shuster, J. C. Stella, and T. G. Whitham.
253 2016. Climate change perils for dioecious plant species. *Nature Plants* **2**:1–8.
- 254 Jones, M. H., S. E. Macdonald, and G. H. Henry. 1999. Sex-and habitat-specific responses
255 of a high arctic willow, *Salix arctica*, to experimental climate change. *Oikos* pages
256 129–138.
- 257 Karger, D. N., O. Conrad, J. Böhner, T. Kawohl, H. Kreft, R. W. Soria-Auza, N. E. Zim-
258 mermann, H. P. Linder, and M. Kessler. 2017. Climatologies at high resolution for the
259 earth's land surface areas. *Scientific data* **4**:1–20.

- 260 Kearney, M., and W. Porter. 2009. Mechanistic niche modelling: combining physiological
261 and spatial data to predict species' ranges. *Ecology letters* **12**:334–350.
- 262 Kindiger, B. 2004. Interspecific hybrids of *Poa arachnifera* × *Poa secunda*. *Journal of*
263 *New Seeds* **6**:1–26.
- 264 Lee-Yaw, A. J., J. L. McCune, S. Pironon, and S. N. Sheth. 2022. Species distribution
265 models rarely predict the biology of real populations. *Ecography* **2022**:e05877.
- 266 Merow, C., S. T. Bois, J. M. Allen, Y. Xie, and J. A. Silander Jr. 2017. Climate change
267 both facilitates and inhibits invasive plant ranges in New England. *Proceedings of the*
268 *National Academy of Sciences* **114**:E3276–E3284.
- 269 Miller, T. E., and A. Compagnoni. 2022. Two-Sex Demography, Sexual Niche Differen-
270 tiation, and the Geographic Range Limits of Texas Bluegrass (*Poa arachnifera*). *The*
271 *American Naturalist* **200**:17–31.
- 272 Morrison, C. A., R. A. Robinson, J. A. Clark, and J. A. Gill. 2016. Causes and conse-
273 quences of spatial variation in sex ratios in a declining bird species. *Journal of Animal*
274 *Ecology* **85**:1298–1306.
- 275 O'Neill, B. C., E. Kriegler, K. L. Ebi, E. Kemp-Benedict, K. Riahi, D. S. Rothman, B. J.
276 Van Ruijven, D. P. Van Vuuren, J. Birkmann, K. Kok, et al. 2017. The roads ahead:
277 Narratives for shared socioeconomic pathways describing world futures in the 21st
278 century. *Global environmental change* **42**:169–180.
- 279 Peterson, A. T., M. Pápes, and J. Soberón. 2015. Mechanistic and correlative models of
280 ecological niches .
- 281 Petry, W. K., J. D. Soule, A. M. Iler, A. Chicas-Mosier, D. W. Inouye, T. E. Miller, and K. A.

- 282 Mooney. 2016. Sex-specific responses to climate change in plants alter population sex
283 ratio and performance. *Science* **353**:69–71.
- 284 Porter, W., S. Ostrowski, and J. Williams. 2010. Modeling animal landscapes. *Physiological*
285 and Biochemical Zoology
- 286 R Core Team, 2023. R: A Language and Environment for Statistical Computing. R
287 Foundation for Statistical Computing, Vienna, Austria. URL <https://www.R-project.org/>.
- 288
- 289 Reed, P. B., S. D. Bridgham, L. E. Pfeifer-Meister, M. L. DeMarche, B. R. Johnson, B. A.
290 Roy, G. T. Bailes, A. A. Nelson, W. F. Morris, and D. F. Doak. 2021a. Climate warming
291 threatens the persistence of a community of disturbance-adapted native annual plants.
292 *Ecology* **102**:e03464.
- 293 Reed, P. B., M. L. Peterson, L. E. Pfeifer-Meister, W. F. Morris, D. F. Doak, B. A. Roy, B. R.
294 Johnson, G. T. Bailes, A. A. Nelson, and S. D. Bridgham. 2021b. Climate manipulations
295 differentially affect plant population dynamics within versus beyond northern range
296 limits. *Journal of Ecology* **109**:664–675.
- 297 Stan Development Team, 2023. RStan: the R interface to Stan. URL <https://mc-stan.org/>.
- 298
- 299 Tognetti, R. 2012. Adaptation to climate change of dioecious plants: does gender balance
300 matter? *Tree Physiology* **32**:1321–1324. URL <https://doi.org/10.1093/treephys/tps105>.
- 302 Vehtari, A., A. Gelman, and J. Gabry. 2017. Practical Bayesian model evaluation using
303 leave-one-out cross-validation and WAIC. *Statistics and computing* **27**:1413–1432.

304 Williams, J. L., H. Jacquemyn, B. M. Ochocki, R. Brys, and T. E. Miller. 2015. Life history
305 evolution under climate change and its influence on the population dynamics of a
306 long-lived plant. *Journal of Ecology* **103**:798–808.